Influence of releases from a fresh water reservoir on the hydrochemistry of the Tinto River (SW Spain).

Carlos Ruiz Cánovas[a, d,*], Manuel Olias[b], Enric Vazquez-Suñé[a], Carlos Ayora[a], Jose Miguel Nieto[c]

[a] Institute of Environmental Assessment and Water Research (IDÆA-CSIC). c/ Jordi Girona 18-26, 08034 Barcelona (Spain)

[b] Department of Physical, Chemical and Natural Systems, University Pablo de Olavide. Ctra.de Utrera km 1, 41013, Sevilla (Spain).

[c] Department of Geology, University of Huelva. Facultad de Ciencias Experimentales, Avenida 3 de Marzo s/n, 21071 Huelva (Spain)

[d] Department of Geodynamics and Paleontology, University of Huelva. Facultad de Ciencias Experimentales, Avenida 3 de Marzo s/n, 21071 Huelva (Spain)

* *Corresponding author:* C.R Cánovas

Department of Geodynamics and Paleontology, University of Huelva. Facultad de Ciencias Experimentales, Avenida 3 de Marzo s/n, 21071 Huelva (Spain)

Tel: +34 959 219 870 ext 1623: Fax: +34 959 219 440

Email: carlos.ruiz@dgeo.uhu.es

Abstract

The Tinto River is an extreme case of pollution by acid mine drainage (AMD), with pH values below 3 and high sulphate, metal and metalloid concentrations along its main course. This study evaluates the impact of releases from a freshwater reservoir on the Tinto River, identifying the metal transport mechanisms. This information is needed to understand the water quality evolution in the long term, and involves the comprehension of interactions between AMD sources, freshwaters, particulate matter and sediments. This work proposes a methodology for quantifying the proportions in which the different sources are contributing. The method is based on the mass balance of solutes and accounts for the uncertainty of end-members. The impact of the releases from the Corumbel Reservoir on the hydrochemistry of the Tinto River was significant, accounting up to a 92% of river discharge. These releases provoked a sharp decrease in dissolved metal concentrations, especially for Fe (approximately 1000 fold) due to dilution and precipitation. Cadmium, Zn, Cu, Co, Ni and Al suffered a dilution to a 12-16 fold decrease while Ca, Sr, Na, Pb and Si were less affected (2-4 folds decrease). However, these releases also gave rise to an increase in particulate transport, mainly Fe, As, Cr, Ba, Pb and Ti, due to sediment remobilisation and Fe precipitation. Aluminium, Li, K, Si, Al, Ni and Sr, together with Cu were present in the particulate phase during the discharge peak. The proposed 2-component mixing model revealed the existence of non-conservative behaviour for Al, Ca, Li, Mn, Ni and Si as a consequence of the interactions between the acidic Tinto waters and the clay-rich reservoir sediments during the bottom outlet opening. These results were improved by a 3-component mixing model, introducing a new end-member to account the chemical dissolution of clay-rich sediments by acidic Tinto waters.

Keywords: acid mine drainage, reservoir releases, mixing processes, particulate pollutants, water quality.

1. Introduction

Owing to the intense mining activities related to concentrations of massive sulphides, many rivers are seriously affected by acid mine drainage (AMD), one of the most important water pollutant processes worldwide. AMD has traditionally been the subject of much research (see reviews by Nordstrom and Alpers, 1999; Johnson and Hallberg, 2005). A review of main factors controlling metal content in AMD affected water courses can be seen in Berger et al. (2000), Lee et al. (2002), Gammons et al. (2005) and Moncur et al. (2005). However detailed studies are still needed to improve the knowledge of water quality evolution in AMD-affected rivers in the long term. A significant improvement of river water quality through dilution during floods is often observed. Cánovas et al. (2008) showed this effect in the Tinto River. In many AMD affected rivers, the urgent need of water resources usually gives rise to the construction of reservoirs in the not contaminated tributaries; however, their influence on the hydrochemistry of these rivers has not been investigated in depth. Reservoirs release water after intense rainfalls take place in order to control floods and, in addition to floods, can play a key role in attenuation of the dissolved pollution. By contrast, the dissolved fraction is not always the predominant carrier phase for metals in rivers. In this sense, metal transport can take place by different mechanisms (Gibbs, 1973): a) in solution; b) adsorbed on solids (organic matter, clays and Fe and Al-hydroxides), where chemical changes are required before releasing, and c) in the crystal structure of mineral particulate, where they are almost unavailable. Achterberg et al. (2003) and Ferris et al. (2004) indicate that metal transport in the Tinto River takes place almost entirely in the dissolved phase. However, both studies do not consider high flow conditions. It is necessary to consider particulate transport provoked by riverbed sediment remobilization and Fe (and others metals) precipitation during these events.

The knowledge of pollutant transport mechanisms in a river affected by AMD relies on understanding the interactions between: (1) AMD affected river water, (2) dilution during floods, (3) discharge of freshwaters (4) reactions with sediment loads and particulate matter. A proper assessment of river water quality involves the identification and quantification of all the sources involved. Despite the importance of such processes, studies of quantitative assessment are lacking. Such type of studies requires the implementation of tools to identify and evaluate the different sources and mixing processes involved in the water quality of a river. Schemel et al. (2000) describe the chemical

transformations and metal transport processes through two mixing zones in the Animas River, Colorado. However, this study, as many traditional mixing ratios computations, requires that the concentrations of end-members are different and accurately known. Actually, the concentrations of the different species in the end-members are not commonly known with certainty. They can be highly variable in space and, especially, time. For these cases is possible to use a methodology (Carrera et al., 2004) for quantifying the proportions in which the different sources are contributing. The method is based on modelling of mixing waters from mass balance of solutes and accounts for the uncertainty of end-members (Carrera et al., 2004; Vázquez-Suñe et al., 2010). Thus, the aim of this work is 1) to identify the metal transport mechanisms, and 2) to evaluate the role played by reservoir releases and floods in the Tinto River water quality.

2. Materials and methods

2.1. Site description

The Tinto River (SW Spain) drains materials belonging to the Iberian Pyrite Belt (IPB), which hosts one of the largest concentrations of massive sulphides in the world (Tornos, 2006). The mineralogical composition of these deposits is dominated by pyrite (FeS_2) with lesser amounts of sphalerite (ZnS), galena (PbS), chalcopyrite ($CuFeS_2$), arsenopyrite (AsFeS) and other sulphides containing accessory metals such as Cd, Co, Ni, Ag, Sn, etc. Owing to the intense mining activities taken place in this area since prehistoric times, the Tinto River is seriously affected by acid mine drainage (AMD).

As a consequence of such intense sulphide oxidation processes, the Tinto River is an extreme case of pollution, with low pH values and high sulphate, metal and metalloid concentrations along its main course (Cánovas et al., 2007). These low pH values are caused by the huge concentrations of Fe, which acts as chemical buffer, maintaining an almost constant pH of around 2.5-3.0 through Fe hydrolysis and subsequently precipitation reactions (Cánovas et al., 2007). The high level of pollution by AMD recorded in the Tinto River, together with the urgent need of water for human consumption in the area, has caused the regulation of its main tributaries. The Corumbel Dam (19 hm^3), located at the lower part of the basin (Fig. 1), is the second reservoir in importance of the catchment, after the Jarrama Dam (43 hm^3), placed at the upper part. The Corumbel Dam has annual average inputs of 28 hm^3, coming from the Corumbel River, which drains material belonging to the PQ group

(phyllites and quartzites) in the northern part and to Neogene in the southern, and accounting for a drainage surface of around 178 km^2.

2.2. Sampling

The sampling site is placed at Gadea, a stream-gauge station belonging to the Andalusian Water Agency, located approximately 41 km downstream of the Riotinto Mining District and around 20 km upstream of its entry into the Ria de Huelva estuary (Fig. 1). The Corumbel Reservoir is located around 5 km upstream of Gadea (Fig. 1).

Sampling was carried out by a Teledyne ISCO® autosampler, with a sample container holding up to 24 bottles and an outlet pipe made of polyethylene. Samples were pumped by a peristaltic pump, with a schedule purge stage between samplings to avoid cross-contamination. Sample-containing bottles were washed in 10% (v/v) nitric acid and then with milli-Q water (18.2 MΩ) prior to sampling. The detailed sampling started on April 24th at 11:00 h, ending on April 26th at 23:00 h. The autosampler was initially programmed to take one sample each hour; however the sampling frequency was changed on April 25th to take one sample every 3 h. Additionally, two samples were collected manually before (21st April) and after (28th April) the detailed sampling. In order to determine dissolved element concentration, all the samples were filtered through 0.45 μm Millipore® Teflon filters, which implies some colloidal particles with lower diameter are considered as dissolved (i.e. Langmuir, 1997). Samples were subsequently acidified with suprapure nitric acid Merk® to pH<2 and stored refrigerated until analysis. As samples were retrieved from the autosampler on a daily basis, there is a delay ranged from minutes to some hours between sample collection and filtration/acidification.

To determine the total element concentration (dissolved + particulate), the nitric acid in-bottle digestion procedure proposed by Garbarino and Hoffman (1999) was followed. This procedure is a modification of a hydrochloric acid in-bottle digestion (Hoffman et al., 1996) used since 1992 by the National Water Quality Laboratory (NWQL) of the U.S Geological Survey (USGS), to determine element concentration in whole water samples. Enough volume of raw water was taken in polyethylene bottles. After adding 1.6 mL of nitric acid for every 50 mL of raw water, each bottle was

capped and vigorously shaken, and subsequently heated in an oven for 8 hours at 65ºC. After removing from the oven, samples were vigorously shaken again and enough volume of the digestate was filtered through 0.45 μm Millipore® Teflon filters. Finally, the filtered aliquots were stored refrigerated until analysis. A reagent blank was prepared with each set of the digested samples.

Temperature, pH, redox potential (Eh) and electrical conductivity (EC) of samples were measured in the field with portable meters (Hanna Instruments HI 9025 and HI 9033). The pH an EC instruments were calibrated before carrying out the readings. Redox potential (Eh) values were corrected to obtain the potential referred to the hydrogen electrode (Nordstrom and Wilde, 1998). Rainfall data were obtained from eight different stations distributed within the Tinto catchment (Fig. 1) while data of water releases from reservoirs and Tinto River discharge were obtained from the Andalusian Water Agency.

2.3. Analysis

Thirty-eight samples were collected during the sampling period, twenty-two of which were selected for analysis of dissolved element concentration. The selecting criterion was significant changes in electrical conductivity (EC) values. Of these, the total concentrations (dissolved + particulate) were determined in thirteen samples. The chemical analyses were undertaken at the Central Research Services of the Huelva University following a custom-designed protocol specific to waters affected by AMD (Ruiz et al., 2003). Cations contained in both the dissolved and total fractions, were analysed using Inductively Coupled Plasma Optical Emission Spectroscopy (ICP-AES) on a Jobin Yvon (JY ULTIMA 2) spectrometer. Aluminium, As, Ba, Ca, Cd, Co, Cr, Cu, Fe, K, Li, Mg, Mn, Na, Ni, Pb, S, Si, Sr, Ti, V and Zn were analysed, although only the most significant elements are presented in this work. Detection limits for major elements were less than 200 μg/L, except for K (310 μg/L). Concerning trace elements, the detection limits for Pb and V were 10 μg/L, 3.2 μg/L for As, and less than 2 μg/L for the rest of elements. A triplicate analysis was performed in order to evaluate the analytical precision, being below 5% in all cases. In each analysis sequence, blanks were analysed, being all elements below the detection limit of the equipment. The analytical accuracy was checked by the analysis of reference materials (NIST-1640).

168 2.4. Data treatment

169 The saturation indices of water samples and the speciation of main elements have been studied
170 using the geochemical code PHREEQC (Parkhurst and Appelo, 1999). The thermodynamic
171 database of PHREEQC was completed with data for the solubility of schwertmannite (Bigham et al.,
172 1996; Yu et al., 1999) and ferrihydrite (MINTEQA2; Allison et al., 1990).

173

174 In order to study the influence in the Tinto River of waters released from the Corumbel Reservoir,
175 the code MIX (Carrera et al., 2004) has been used. This software can be freely downloaded from
176 http://www.h2ogeo.upc.es/software/MIX_PROGRAM/index.htm. MIX is a maximum likelihood
177 method to estimate mixing ratios, while acknowledging uncertainty in end-member concentrations.
178 Maximizing the likelihood of concentration measurements with respect to both mixing ratios and end-
179 member concentrations leads to a general constrained optimization problem. The variables need
180 satisfying some conditions to be suitable in mixing models: exhibit a conservative behaviour and their
181 values must be significantly different in the extreme components. This method also allows
182 formulating hypothesis on the geochemical reactions responsible of the non-conservative behaviour
183 in elements.

184

185 ## *3. Results and Discussion*

186 3.1. Description and relative contribution of discharges

187 During the study period rainfalls close to 25 mm were registered. The Tinto River contribution during
188 this period was around 1.1 hm^3, a 9% of the Tinto River discharge in the hydrological year 2005/06
189 (Cánovas, 2009). A manual sample was taken on April 21st, coinciding with a total rainfall below 2
190 mm, which had not influence on the river discharge (Fig. 2A). Rainfall was more intense on April 23rd
191 (19 mm) provoking a maximum discharge value of 7.5 m^3/s on April 24th. The autosampling begun
192 on 24th, before the discharge peak, thus only a limited number of samples could be taken during the
193 rising limb of the hydrograph (Fig. 2A). Later, the discharge decreased progressively down to 0.45
194 m^3/s on April 28^{th,} when the sampling ends.

195

196 This rise in discharge recorded was not only due to the rainfalls; from April 23rd to 27th the Corumbel
197 Reservoir released 1.3 hm^3 of water (Fig. 2B) a value slightly higher than that recorded at the gauge

198 station, which suggests a discharge underestimation of the gauging system. The importance of these
199 releases through the spillway was higher on April 23rd and 24th with an average of 3.6 and 8.3 m^3/s,
200 respectively (Fig. 2B). From April 25th on, spillway releases decreased progressively. On April 26th
201 and 27th a part of discharges was released from the bottom outlet (Fig. 2B). Finally, releases from
202 the Corumbel Reservoir ceased on April 27th.
203
204 3.2. Dissolved concentrations
205 The evolution of pH, EC and some dissolved elements during the study period is shown in Figure 3.
206 A marked drop in EC (from 2.5 to 0.34 mS/cm) and a rise in pH values (from 2.6 to 4.4) is observed
207 concomitant to the discharge peak (Fig. 3) Later, EC increased progressively coinciding with a
208 decrease in pH values, although this tendency was interrupted on April 25th, when a pH rise and a
209 slight EC drop was recorded (Fig. 3). However, the most striking observation was the sharp increase
210 in EC (maximum of 1.6 mS/cm) recorded on April 26th, concurrently with a decrease in pH values (up
211 to 2.9). Finally, EC and pH values seem to remain almost constant around 1.0 mS/cm and 3.0,
212 respectively, until the end of the study period.
213
214 Most elements decreased their concentration during the rise in discharge, coinciding with the
215 maximum value of pH (Fig. 3). The minimum values of sulphate and metal concentrations reached
216 are quite low; 129 mg/L of sulphate, 4.4 mg/L of Al, 1.3 mg/L of Cu and Zn, etc. Iron, Cr and Pb
217 concentrations were even below the detection limit of the equipment. If comparing concentration
218 values observed during the hydrograph peak to pre-event values, Fe was the element which suffered
219 a higher decrease (approximately 1000 fold, from 139 to less than 0.15 mg/L). The concentration of
220 Co, Ni, Cd, Zn, Cu and Al suffered between a 12 and 16 fold decreases, meanwhile sulphate, Mg
221 and Mn did between 7 and 10. Strontium, Ca, Na, Pb and Si followed the lowest decrease (between
222 a 2 and 4 fold). The only element which increased during the discharge peak was Ba.
223
224 According to its behaviour, elements can be grouped into four families following a different evolution.
225 • F1 formed by Cd, Fe, Zn and sulphate (Fig. 3), characterised by reaching the highest
226 concentration at the beginning of the controlled period.

- F2 formed by Ca, Al, Li, Si, Sr, Mn and Ni (Fig. 3), which exhibited its highest value during the bottom outlet releases (in the case of Al was similar to that found at the beginning of the controlled period) and, once the releases are interrupted, its concentration tends to decrease.
- F3, formed by EC, Co and Mg (Fig. 3), characterised by a sharp increase in concentration during the reservoir bottom outlet releases, as elements of F2. However, the concentration decrease observed for this group after the end of releases was not so marked as for F2.
- F4, formed by Cu and Pb (Fig. 3), which did not experiment the increase observed for other elements during the bottom outlet releases (the Pb concentration peaks during the spillway release on April 25th), showing instead lower values during these releases (Fig. 3).

A different behaviour was followed by other elements such as Na, Ba and Ti, which could not be included in any group. The concentration of Na decreased initially in response to the rise in discharge, recovering progressively after the discharge peak (Fig. 3). Barium increases its concentration with the water releases while Ti concentration fluctuates through the event without an appreciably tendency (not shown in Fig. 3).

3.3. Total concentrations

Analyses of total concentrations (dissolved + particulate) reveal the relevance of particulate transport for As, Ba, Cr, Fe, Pb, Ti and V (Figs. 4 and 5). Thus, elements like As, which showed low dissolved concentrations (close to the detection limit), reached high total concentrations with a median value of 2,547 µg/L. Just the opposite can be appreciated for a group of elements formed by Ca, Cd, Na, Zn, Mn, Mg and Co, which were chiefly transported in the dissolved phase (Fig. 5). A third group (Cu, Li, K, Si, Al, Ni, Sr and sulphate) shows an intermediate behaviour, although K and Si show more affinity for the particulate phase while Cu, Ni, Sr and Li tend to be in the dissolved one.

Hudson-Edwards et al. (1999) identify jarosite, plumbojarosite and possibly schwertmannite as the most common minerals in alluvium downstream of the Riotinto Mining District (Fig. 1). These Fe mineral phases are the major host of trace metals in the Tinto River, retaining most of the As, Cr and Pb contained in riverbed sediments (Galán et al., 2003). Lead is deeply affected by coprecipitation

257 processes in the Tinto River (Cánovas et al., 2007) provoking a Pb enrichment in riverbed sediments.
258 The rapid removal of As and V close to AMD sources by sorption or coprecipitation processes on Fe
259 mineral phases has been documented in the region (Sanchez España et al., 2006; Acero et al.,
260 2006; Asta et al., 2010).
261
262 On the other hand, the sediment load suspended in the Tinto River is largely composed of clay
263 minerals (mica, kaolinite and chlorite) with significant amounts of quartz, feldspars, and locally
264 jarosite, hematite and carbonates (Galán et al., 1999). The presence of Al, Li, K, Si, Ni and Sr in
265 these mineral phases is abundant.
266
267 3.4. Hydrogeochemical characterisation and mixing processes
268 The hydrochemical evolution of the Tinto River during the controlled period is strongly marked by the
269 arrival of waters released from the Corumbel Reservoir. Two different types of waters came into
270 contact during the study period, the acidic and metal rich waters (139 mg/L of Fe, 72 mg/L of Al, 20
271 mg/L of Cu, etc.; Pre-event water, Table 1) from the Tinto River and the circumneutral and low
272 mineralized waters from the Corumbel Reservoir (Table 1).
273
274 The great influence of the Corumbel Reservoir on the Tinto River hydrochemistry is evident according
275 to the volume of water released in relation with the river discharge and the low dissolved metal
276 concentration recorded during this flood. The median for Fe is only 3.3 mg/L; an extremely low value
277 compared with the annual median (81 mg/L) recorded in the Tinto River downstream the junction
278 (Cánovas et al., 2007). With a discharge peak of 7.5 m^3/s during this flood, lower concentrations than
279 those observed in the flood of October 2004 (reaching discharges higher than 100 m^3/s; Cánovas et
280 al., 2008) were recorded. The mixing of Tinto waters with the non-polluted reservoir waters provoked
281 a dilution effect, which notably improved the Tinto water quality. The lowest element concentrations
282 were reached during the discharge peak while concentrations recovered during the falling limb.
283 However, some fluctuations in water mineralization can be observed (Fig. 3). These changes may
284 be due to the arrival of waters of variable mineralization coming from the farther parts of the
285 catchment, which provokes hysteresis in the relation between metal content and river discharge
286 (Evans and Davies, 1998; Cánovas et al., 2010). However, not all elements followed a similar

287 evolution during these changes in water mineralization as shown in section 3.2. In this way, the
288 increase in most element concentrations observed on April 26th was unusually important for some
289 elements (i.e. Al, Ca, Co, Li, Ni, Si, Sr) that suggests the influence of other factors.
290
291 The mixing of Corumbel freshwaters with the acidic and Fe-Al rich Tinto waters led to Fe hydrolysis
292 reactions. These reactions liberated acidity and buffered the pH (maximum value of 4.4; Fig. 3),
293 despite the huge volume of fresh-waters released from the Corumbel Reservoir. Figure 6 shows a
294 sharp decrease of Fe/SO_4 mass ratios after the discharge rise (day 24th). This is attributed to the
295 precipitation of Fe mineral phases, probably schwertmannite (Table 2) as this mineral phase seems
296 to control the pH between 2 and 4 in the region (Sánchez-España et al., 2005; Cánovas et al., 2008;
297 Sarmiento et al., 2009; Cánovas, 2009).
298
299 The buffering effect exerted by Fe remains until Fe(III) is depleted. Then, Al can replace Fe(III) as
300 buffering agent (Nordstrom and Alpers, 1999). The low concentrations of Fe (even below the
301 detection limit of the equipment) reached during the event could suggest the depletion of Fe and its
302 replacement by Al as buffering agent. The decrease of Al/SO_4 mass ratio, however, is not as evident
303 as for Fe/SO_4 (Fig. 6). In fact, jurbanite was the only Al mineral phase close to equilibrium (Table 2),
304 and despite its apparent thermodynamic stability this mineral rarely precipitates in environments
305 affected by AMD (Bigham and Nordstrom, 2000; Blowes et al., 2005). A significant increment of
306 hydroxyl containing Al complexes was not observed either. In this sense, the sulphate complex
307 $AlSO_4^+$ remained as dominant Al specie after the discharge rise (PHREEQC calculations not shown).
308 This would indicate that, unlike Fe, Al seems not to have a relevant role in pH buffering during the
309 event.
310
311 All elements were not equally affected during the mixing processes. Elements from group F2 (Cu,
312 Cd, Zn, Ni, Al, etc.) decreased their concentration at a lesser extent than Fe as they were not affected
313 by precipitation and sorption is not expected at such low pH values; therefore, they may be only
314 affected by dilution. The elements from the Tinto River that suffered the lowest decrease in
315 concentration were Pb, Sr, Ca, Na and Si. Strontium, Ca, Na and Si show significant concentrations
316 in Corumbel waters (Table 1). Lead concentration was already low in the Tinto River. This element

317 does not decrease with the increase in Fe particulate probably because, unlike jarosite, it is not
318 incorporated to schwertmannite (Acero et al., 2006; Table 2).
319
320 The increase in most element concentrations observed in April 26th was unusually important for some
321 elements no typical of AMD, mainly belonging to family F2 and at a lesser extent F3 (Al, Ca, Li, Mn,
322 Ni, Sr), which suggests the influence of other factors. This anomalous increase coincides with the
323 opening of the bottom outlet releases of the Corumbel Dam. Mediterranean climate rivers have high
324 sediment yields which are trapped by regulating reservoirs. The bottom outlets are seasonally
325 opened to dredge bottom sediments in order to avoid the dam colmation, which causes a huge
326 increase of suspended matter downstream of the dams. These sediments are fine grained size,
327 mainly clays, as sediments tend to be deposited along the dam according to an inverse granulometric
328 sequence: the coarser fraction is deposited in the tail while the finer is progressively settled close to
329 the dam.
330
331 The interaction between the acidic Tinto waters and the reservoir clay-rich sediments would produce
332 the dissolution of these suspended particles and an increase in concentration of Al, Ca, Mn, Ni, Si,
333 etc. Galán et al. (1999) investigated the acid dissolution of representative phyllosilicate samples by
334 Tinto waters, showing the total dissolution of smectite and the structural alteration of chlorite within
335 the first 30 minutes of water-mineral contact. As well as smectite, the calcite contained in sediment
336 samples was totally dissolved during the first 30 minutes, releasing Ca into solution and raising the
337 pH (Galán et al., 1999). The dissolution of these minerals also causes a slight increase in
338 concentration of Fe, Cu, etc. as they are present as accessory elements in these phases.
339
340 Mixing processes also affected the particulate load transported by the river. In this sense, Fe, As, Cr,
341 Ba, Pb, Ti and V were mainly carried by the particulate matter. Particulate Fe was almost 100 times
342 higher than dissolved (Fig. 4). The precipitation of dissolved Fe during the event cannot account for
343 such high amount of particulate Fe. At this respect, water releases from the Corumbel Reservoir
344 must remobilise high amounts of Fe rich precipitates previously deposited on the riverbed, being
345 subsequently transported by the river. These precipitates also contain high concentrations of As, Ba,
346 Cr, Pb (Hudson Edwards et al., 1999; Galán et al. 2003)

347

348 3.5. Mixing model

349 In order to study the influence of the waters released from the Corumbel Reservoir, the code MIX
350 (Carrera et al., 2004) has been used. Pre-event Tinto and Corumbel reservoir waters (Table 1) were
351 selected as end-members. The initial assumption is that the mixing of both types of waters explains
352 the variability in river water composition. The total discharge carried by the river at the sampling point
353 will be the sum of the base flow carried by the Tinto River before joining the Corumbel River with the
354 volume of water released from the Corumbel reservoir (Fig. 1). As the quality of MIX computations
355 improves increasing the number of variables and samples analyzed, 14 variables which seem to
356 have a quasi-conservative behaviour were considered; EC, Al, Ca, Cd, Co, Li, Mg, Mn, Na, Ni, Si,
357 Sr, sulphate and Zn.

358

359 The mixing ratios computed by MIX evidence a great influence of water releases from the Corumbel
360 Reservoir on the Tinto River hydrochemistry during the event. Reservoir waters yielded around 92%
361 of Tinto River discharge at the beginning, fluctuating up to the end of the event (Fig. 7). The obtained
362 results show very good correlations ($R^2 \geq 0.98$) between measured and estimated values for EC, Mg
363 and sulphate while the rest (Al, Ca, Li, Mn, etc.) show lower correlations, as the values measured in
364 the more concentrated samples generally are higher than those estimated by MIX. These elements
365 reached its highest concentration during the bottom outlet release. The samples which shows
366 deviation between measured and estimated values corresponds to the increase in concentration on
367 April 26th (Fig. 3). As it has been commented previously, during the opening of the bottom outlets a
368 high amount of fine grained size sediments is released from the bottom reservoir into the river. The
369 interaction between the acidic Tinto waters and this reservoir clay-rich sediment may produce the
370 dissolution of these suspended particles and increase the concentration of Al, Ca, Mn, Ni, Si, etc

371

372 Therefore, a third end-member to explain the hydrochemistry variations during the event is proposed;
373 the clay-rich sediment loaded waters coming from the bottom outlets. This is more an approach to
374 explain the mixing model than a realistic solution itself, what this end-member represents is the
375 chemical process of acid attack of reservoir bottom sediments by Tinto waters. In order to obtain the
376 chemical composition for this end-member a mass balance has been performed, assuming the

discharge data and the concentrations of all components. The MIX method (Carrera et al., 2004) yields improved estimates of end-members concentration (Table 1), acknowledging some uncertainty in initial concentrations. Values obtained from mass balance for clay dissolution end-member were very similar to those estimated by MIX (Fig. 8). As this third end-member is caused by opening of the bottom outlets in Corumbel Reservoir on April 26th, the influence of the third end-member is only restricted to samples taken after this date. The results obtained from this 3-component mixing model show better correlations between measured and estimated values for most variables (Fig. 8).

4. Conclusions

The Tinto River is famous worldwide due to the extreme conditions recorded through the year, with pH values lower than 3 and huge sulphate and metal concentrations. However, during the controlled period (from April 24th to 28th) the pH reached values above 4 and low metal concentrations were found as a consequence of water releases from the Corumbel Dam (accounting up to 92% of Tinto River discharge). The impact in the resulting water composition is notorious; Fe was the element which suffered a higher decrease (approximately 1000 fold, from 139 to less than 0.15 mg/L) due to both the dilution effect of waters released from the Corumbel Reservoir and Fe precipitation.

Other elements such as Co, Ni, Cd, Zn, Cu and Al decreased at a lesser extent, between a 12 and 16 fold decrease, being dilution the only process controlling their concentrations. Strontium, Ca, Na and Si (together with Pb) followed the lowest decrease in concentration, between a 2 and 4 fold decrease, due to their greater concentration in the waters of the Corumbel Reservoir.

It is clear the importance of particulate transport during the event provoked by both riverbed sediment remobilization and Fe precipitation. A group of elements formed by Fe, As, Cr, Ba, Pb, Ti and V were mainly carried in the particulate matter. Particulate Fe was almost 100 times higher than dissolved. These Fe mineral phases are the major host of trace metal/metalloids in the Tinto River, retaining most of As, Cr, V and Pb. On the other hand, Ca, Cd, Na, Zn, Mn, Mg and Co are chiefly transported in the dissolved phase. Aluminium, Li, K, Si, Al, Ni and Sr, together with Cu showed an intermediate behaviour, being transported in both the dissolved and particulate phases.

In this study, a new tool to study the influence of mixing processes on the hydrochemical behaviour of the river has been successfully implemented. The variability in the river water composition during this event is explained by means of a 2-component mixing model computed by MIX methodology. The good correlation between measured and estimated values for EC, Co, Mg and sulphate would confirm the goodness of the proposed mixing model. However, a group of elements (Al, Ca, Li, Mn, Ni and Si) did not show a good correlation due to an underestimation in the more concentrated samples. The collection of these samples coincides with the opening of the bottom outlets of the Corumbel Reservoir. This operation releases a huge load of fine grained sediments, mainly clays, into the Tinto River which dissolution by its acidic water would be the main source of Al, Ca, Li, Mn, etc. These results are improved by a 3-component mixing model, introducing a new end-member to account the chemical dissolution of clay-rich sediments by acidic Tinto waters.

Acknowledgements

This work has been financially supported by the Spanish Government Project CGL2010-21956-C02). The Andalusian Water Agency is gratefully acknowledged for providing water discharge and releases data from the Corumbel Reservoir.

References

Acero P, Ayora C, Torrentó C, Nieto JM. The behavior of trace elements during schwertmannite precipitation and subsequent transformation into goethite and jarosite. Geochim Cosmochim Acta 2006; 70: 4130-4139.

Achterberg EP, Herzl VMC, Braundgardt CB, Millward CE. Metal behaviour in an estuary polluted by acid mine drainage: the role of particulate matter. Environ Pollut 2003; 121: 283-292.

Allison JD, Brown DS, Novo-Gradac KJ. MINTEQA2/PRODEFA2. A geochemical assessment model for environmental systems. Version 3.0. Athens (Georgia): Environmental Research Laboratory, Office of Research and Development, U.S. Environmental Protection Agency; 2003.

439 Asta MP, Ayora C, Román-Ross G, Cama J, Acero P, Gault AG, Charnock JM, Bardelli,F. Natural
440 attenuation of arsenic in the Tinto Santa Rosa acid stream (Iberian Pyritic Belt, SW Spain):
441 The role of iron precipitates. Chem Geol 2010; 271: 1-12.
442 Berger AC, Bethke CM, Krumhansl ML. A process model of natural attenuation in drainage from a
443 historic mining district. Appl Geochem 2000; 15: 655-666.
444 Bigham JM, Schwertmann U, Traina SJ, Winland RL, Wolf M. Schwertmannite and the chemical
445 modeling of iron in acid sulfate waters. Geochim Cosmochim Acta 1996; 60(12): 2111-2121.
446 Bigham JM, Nordstrom DK. Iron and Aluminium Hydroxysulfate Minerals. In: Alpers CN, Jambor JL,
447 Nordstrom DK, editors. Sulfate Minerals.Crystallography, Geochemistry and Environmental
448 Significance. Reviews in Mineralogy and Geochemistry, v.40. Washington D.C:
449 Mineralogical Society of America; 2000. p. 351-403
450 Blowes DW, Ptacek CJ, Jambor JL, Weisener CG. The geochemistry of acid mine drainage. In: Lollar
451 B.S, editor. Treatise on geochemistry. Environmental geochemistry, 9: Oxford: Elsevier;
452 2005. p. 149-204.
453 Cánovas CR, Olías M, Nieto JM, Sarmiento AM, Cerón JC. Hydrogeochemical characteristics of the
454 Odiel and Tinto rivers (SW Spain). Factors controlling metal contents. Sci Total Environ 2007;
455 373: 363-382.
456 Cánovas CR, Hubbard CG, Olías M, Nieto JM, Black S, Coleman ML. Hydrochemical variations and
457 contaminant load in the Río Tinto (Spain) during flood events. Jour Hydrol 2008; 350 (1-2):
458 24-40.
459 Cánovas CR. La calidad del agua de los ríos Tinto y Odiel. Evolución temporal y factores
460 condicionantes de la movilidad de los metales. Ph.D Thesis. University of Huelva 2009.
461 Available via http://hdl.handle.net/10272/604. Accessed 8 Nov 2009.
462 Cánovas CR, Olías M, Nieto JM, Galván L. Wash-out processes of evaporitic sulfate salts in the
463 Tinto river: Hydrogeochemical evolution and environmental impact. Appl Geochem 2010; 25
464 (2): 288-301.
465 Carrera J, Vázquez-Suñé E, Castillo O, Sánchez-Vila X. A methodology to compute mixing ratios
466 with uncertain end-members. Water Resour Res 2004; 40: W12101, 11 p.
467 Evans C, Davies TD. Causes of concentration/discharge hysteresis and its potential as a tool for
468 analysis of episode hydrochemistry. Water Resour Res 1998; 34: 129-137.

469 Ferris FG, Hallbeck L, Kennedy CB, Pedersen K. Geochemistry of acidic Rio Tinto headwaters and
470 role of bacteria in solid phase metal partitioning. Chem Geol 2004; 212: 291-300.
471 Galán E, Gómez-Ariza JL, González I, Fernández-Caliani JC, Morales E, Giráldez I. Heavy metal
472 partitioning in river sediments severely polluted by acid mine drainage in the Iberian Pyrite
473 Belt. Appl Geochem 2003; 18: 409-421.
474 Galán E, Carretero MI, Fernández-Caliani JC. Effects of acid mine drainage on clay minerals
475 suspended in the Tinto River (Rio Tinto, Spain), an experimental approach. Clay Miner 1999;
476 34 (1): 99-108.
477 Gammons CH, Nimick DA, Parker SR, Cleasby TE, McCleskey RB. Diel behaviour of iron and other
478 heavy metals in a mountain stream with acidic to neutral pH: Fisher Creek, Montana, USA.
479 Geochim Cosmochim Acta 2005; 69: 2505–2516.
480 Garbarino JR, Hoffman GL. Methods of analysis by the U.S. Geological Survey National Water
481 Quality Laboratory. Comparison of a nitric acid in-bottle digestion procedure to other whole-
482 water digestion procedures. Open File Report 99-094. Denver (Colorado): US Geological
483 Survey; 1999.
484 Gibbs RJ. Mechanisms of trace metal transport in rivers. Science 1973; 180 (4081): 71-73.
485 Hoffman GL, Fishman MJ, Garbarino JR. Methods of analysis by the U.S. Geological Survey National
486 Water Quality Laboratory. In-bottle acid-digestion of whole-water samples. Open file report
487 96-225. Denver (Colorado): US Geological Survey; 1996.
488 Hudson-Edwards KA, Schell C, Macklin MG. Mineralogy and geochemistry of alluvium contaminated
489 by metal mining in the Rio Tinto area, southwest Spain. Appl Geochem 1999; 14: 1015-1030.
490 Johnson D, Hallberg K. Acid mine drainage remediation options: a review. Sci Total Environ 2005;
491 338: 3-14
492 Lee G, Bigham JM, Faure G. Removal of trace metals by coprecipitation with Fe, Al and Mn from
493 natural waters contaminated with acid mine drainage in the Ducktown Mining District,
494 Tennessee. Appl Geochem 2002; 17: 569-581.
495 Moncur MC, Ptacek CJ, Blowes DW, Jambor JL. Release, transport and attenuation of metals from
496 an old tailing impoundment. Appl Geochem 2005; 20: 639-659.

497 Nordstrom DK, Wilde FD. Reduction–oxidation potential (electrode method). National field manual
498 for the collection of water quality data. In: Wilde FD, Radtke DB, Gibbs J, Iwasubo RT. U.S.
499 Geological Survey techniques of water-resources investigations, book 9: 1998. A6.5.
500 Nordstrom DK, Alpers CN. Geochemistry of acid mine waters. In: The environmental geochemistry
501 of mine waters. Rev econ geol., 6A; 1999. p. 133-160.
502 Parkhurst DL, Appelo CAJ. User's guide to PHREEQC- A computer program for speciation, reaction-
503 path transport, and inverse geochemical calculations. Water Resources Investigations
504 Report 99-4259: US Geological Survey; 1999
505 Ruiz MJ, Carrasco R, Pérez-López R, Sarmiento AM, Nieto JM. Calibración de un estándar natural
506 para el análisis de muestras de drenaje ácido de minas (AMD) mediante UN-ICP-OES.
507 Proceedings IV Iberian Geochemical Meeting, 14–18 Julio 2003. Coimbra, Portugal.
508 University of Coimbra. 414- 416.
509 Sánchez-España J, Lopez Pamo E, Santofimia E, Aduvire O, Reyes J, Barettino D. Acid mine
510 drainage in the Iberian Pyrite Belt (Odiel river watershed, Huelva, SW Spain): Geochemistry,
511 mineralogy and environmental implications. Appl Geochem 2005; 20: 1320-1356.
512 Sarmiento AM, Olías M, Nieto JM, Cánovas CR. Hydrochemical characteristics and seasonal
513 influence on the pollution by acid mine drainage in the Odiel river Basin (SW Spain). Appl
514 Geochem 2009; 24: 697-714.
515 Schemel LE, Kimball BA, Bencala KE. Colloid formation and metal transport through two mixing
516 zones affected by acid mine drainage near Silverton, Colorado. Appl Geochem 2000; 15:
517 1003-1018.
518 Tornos F. Environment of formation and styles of volcanogenic massive sulfides: The Iberian Pyrite
519 Belt. Ore Geol Rev 2006; 28 (3): 259-307.
520 Vázquez-Suñé E, Carrera J, Tubau I, Sánchez-Vila X, Soler A. An approach to identify urban
521 groundwater recharge. Hydrol Earth Syst Sci 2010; 14, 2085-2097.
522 Yu JY, Heo B, Choi IK, Cho JP, Chang HW. Apparent solubilities of schwertmannite and ferrihydrite
523 in natural stream waters polluted by mine drainage. Geochim Cosmochim Acta 1999;
524 63(19/20): 3407-3416.
525
526

FIGURE CAPTIONS

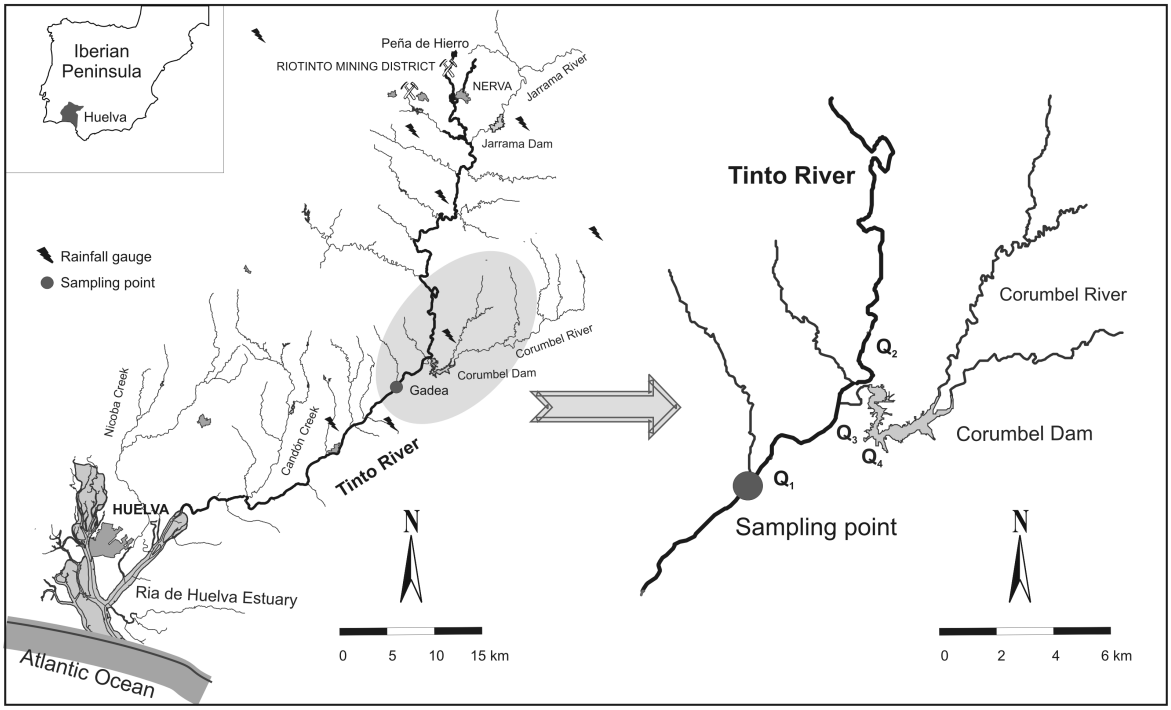

Figure 1. Location map of the Tinto River, indicating the sampling point, the Corumbel Reservoir, the Riotinto Mining District, rainfall stations and the different river contributions during the event.

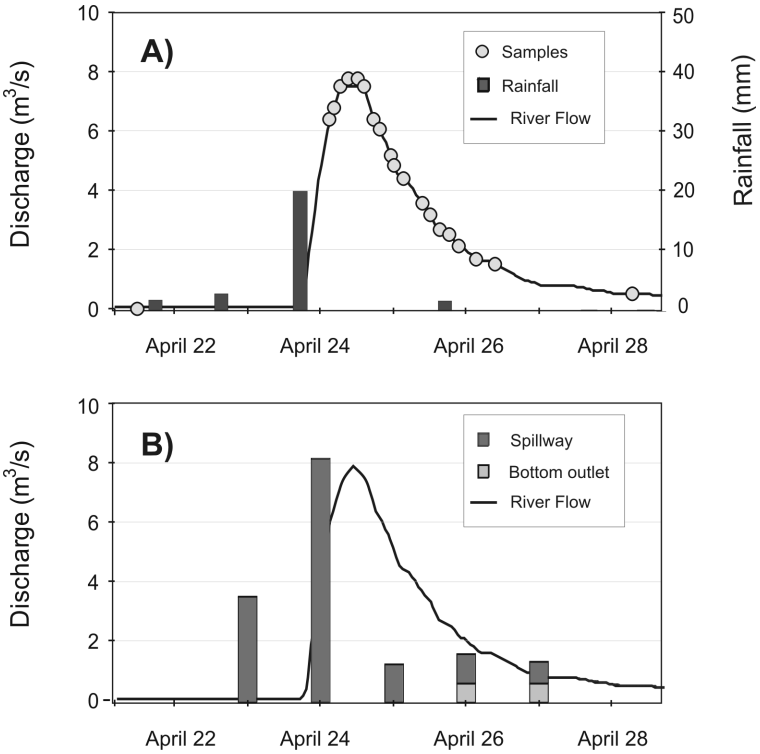

Figure 2. A) Rainfall distribution, river flow and water samples during the monitored period,; B) Releases from the Corumbel Reservoir in relation to the Tinto River flow.

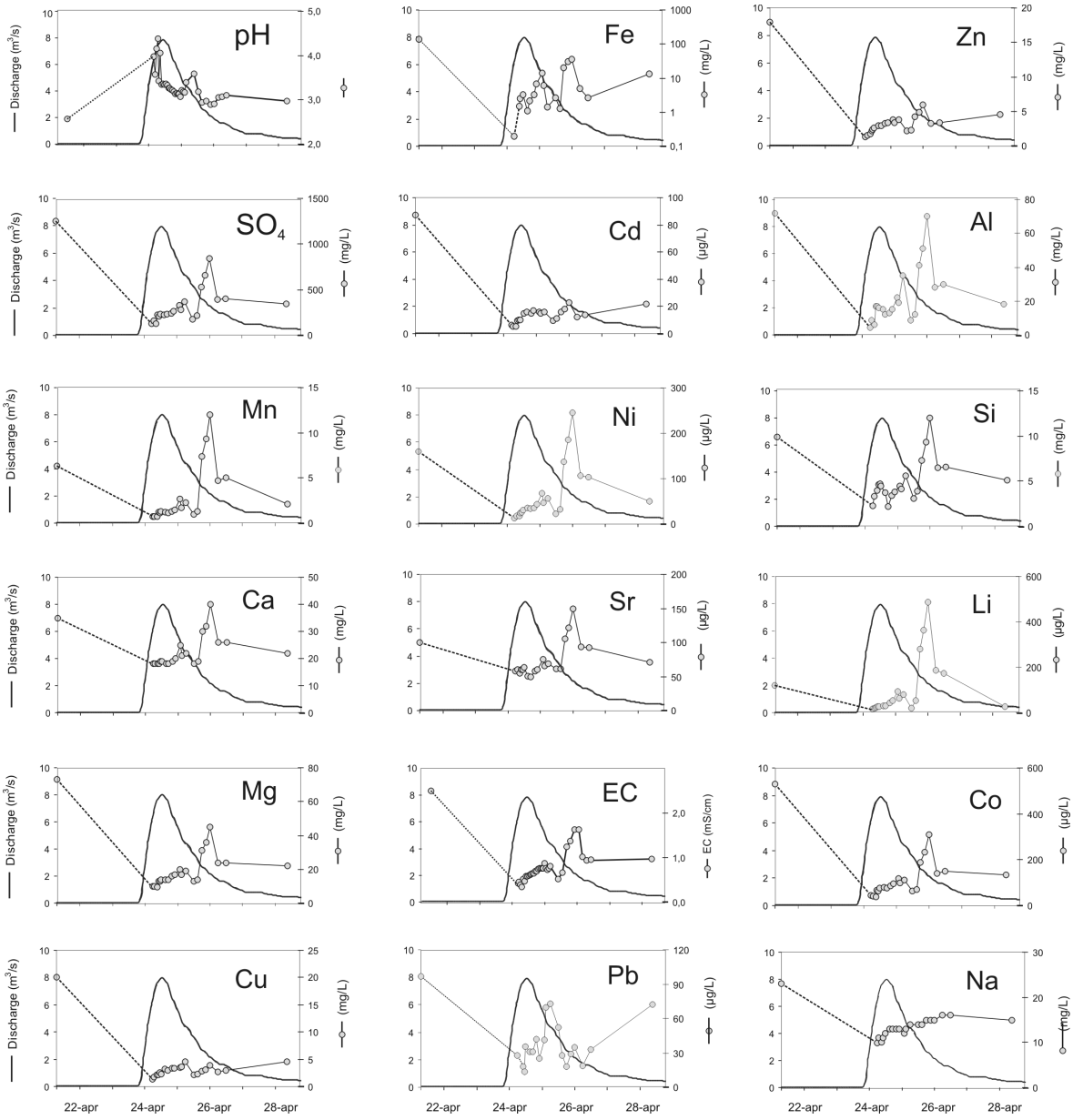

Figure 3. Evolution of dissolved elements during the controlled period.

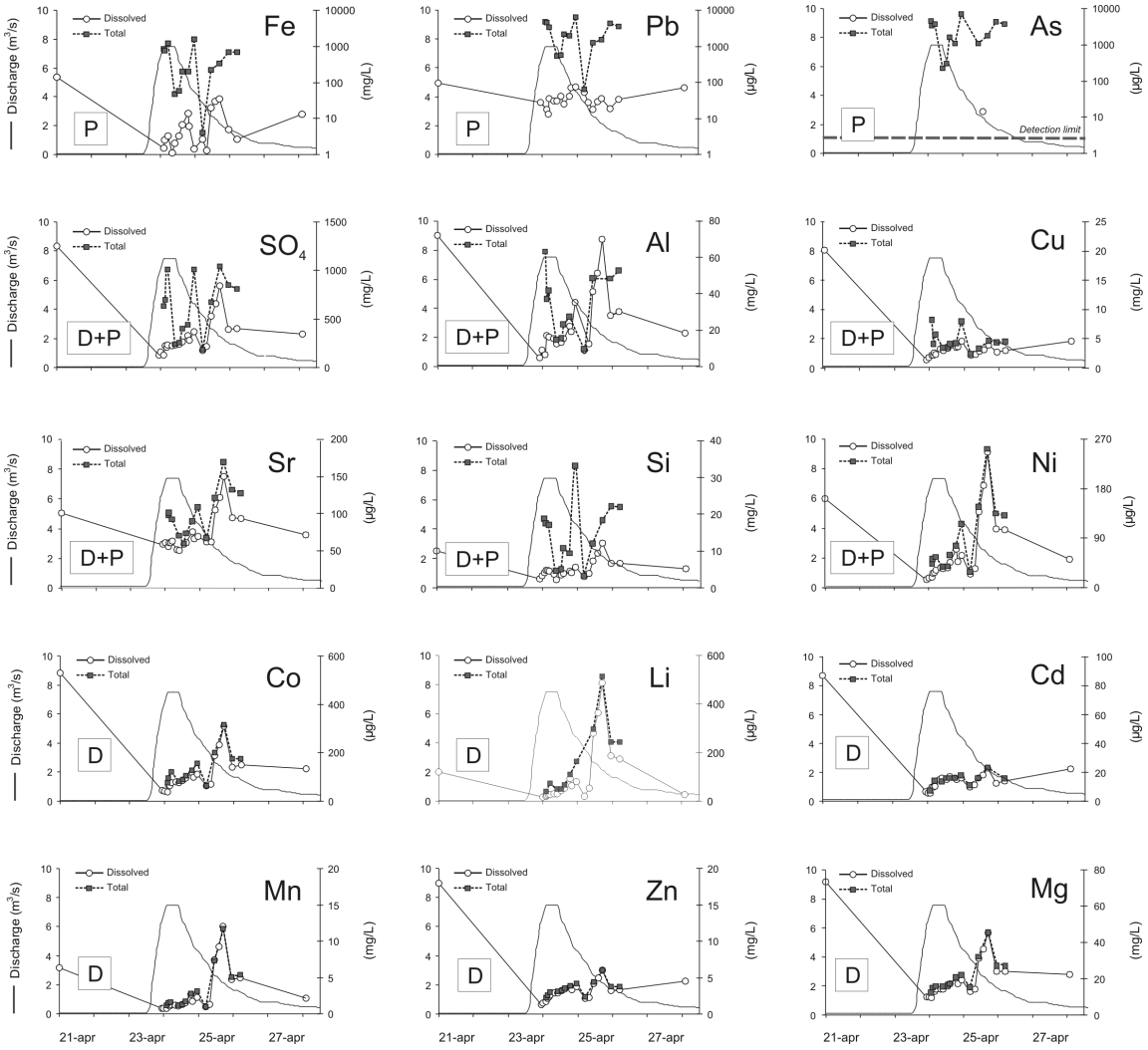

Figure 4. Comparison between the dissolved and total concentration of some selected elements during the event. Legend: P= mainly in particulate phase; D= mainly in aqueous phase; D+P= mixed.

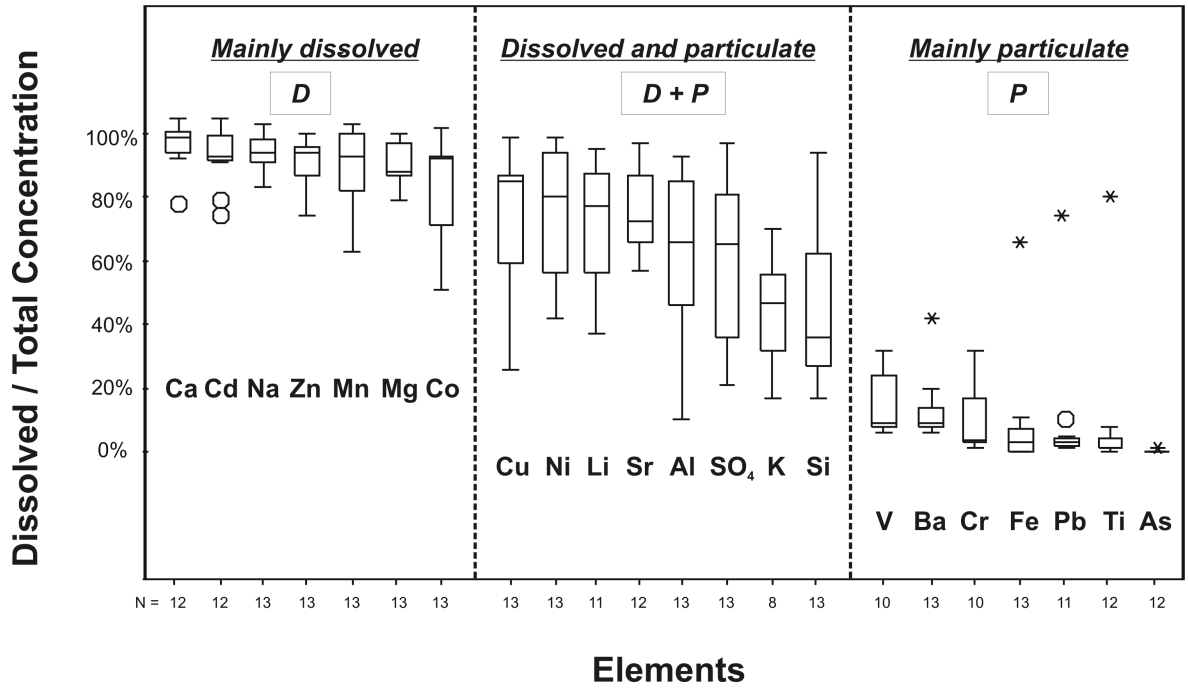

Figure 5. Box-plot indicating the element distribution between dissolved and particulate phase during the event.

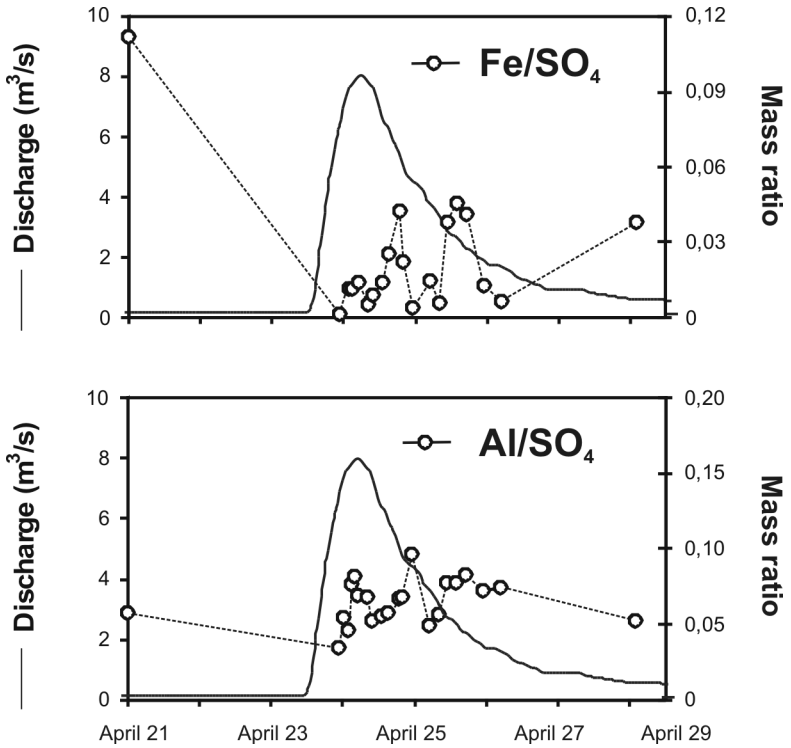

Figure 6. Variation of Fe and Al concentrations with respect to SO_4, considered quasi conservative during the controlled event.

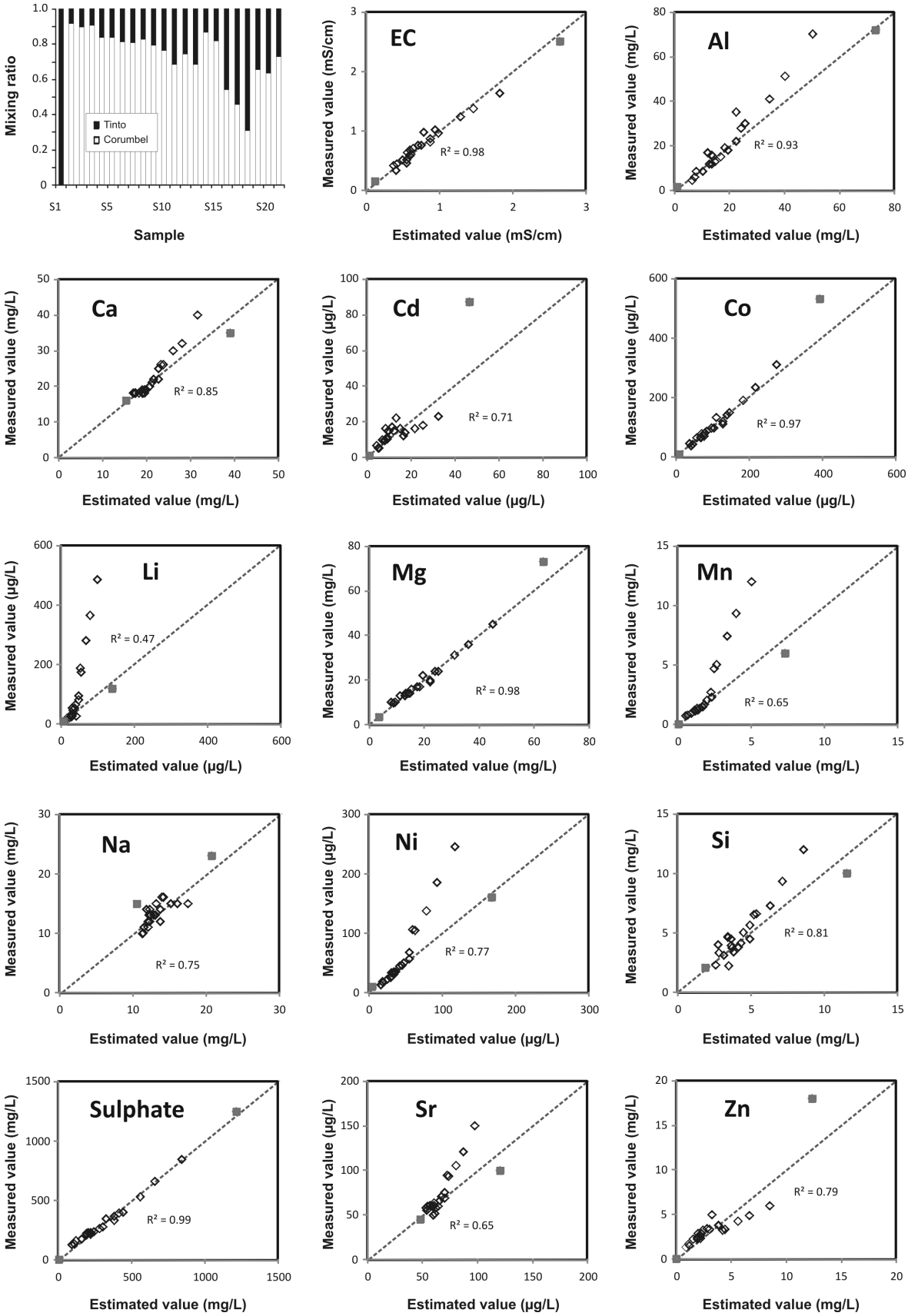

Figure 7. Results obtained from the MIX computation in a 2-component mixing model, using pre-event Tinto and Corumbel waters as end-members. Samples and end-members correspond to grey and white squares, respectively.

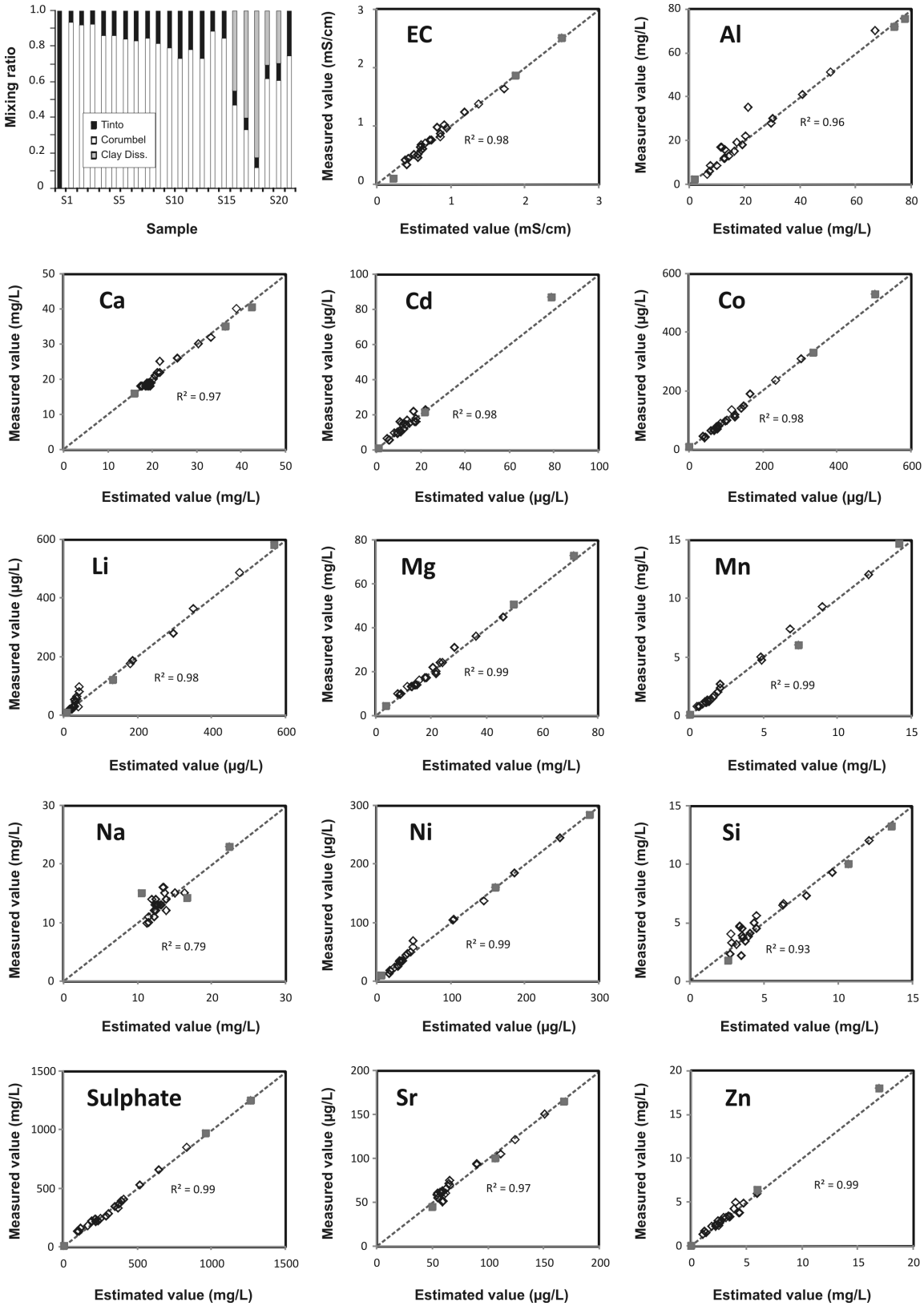

Figure 8. Results obtained from the MIX computation in a 3-component mixing model, adding as third end-member the solution of reservoir sediment acid attack obtained by mass-balance. Samples and end-members correspond to grey and white squares, respectively.

584 TABLE CAPTIONS

585

		End-Members used in MIX computations		
		Tinto River (TR)	*Corumbel water (CW)*	*Clay dissolution (CD)*
		Q_2	Q_3	Q_4
EC	mS/cm	2,50	0,10	1,87
Al	mg/L	72	0,2	75
Ca	mg/L	35	26	41
Co	µg/L	530	10	332
Cd	µg/L	87	1,0	21
Li	µg/L	120	9,0	582
Mg	mg/L	73	5,9	51
Mn	mg/L	6,0	0,05	15
Na	mg/L	23	13	14
Ni	µg/L	160	10	284
Si	mg/L	10	1,7	13
SO_4	mg/L	1248	9,6	969
Sr	µg/L	100	62	165
Zn	mg/L	18	0,01	6,4

586

587 Table 1. End-members used in MIX computations.

588

589

Mineral phase	Pre-Event	Event	Mineral phase	Pre-Event	Event
$Fe(OH)_3$ (a)	-1,5	-1,2			
JarositeH	-0,5	-3,5	Anglesite	-1,6	-2,0
Jarosite-K	-	-0,1	Anhydrite	-1,6	-2,0
Jarosite-Na	-0,8	-3,2	Barite	0,0	0,1
Jarosite-Pb	2,2	0,0	Celestine	-2,2	-2,6
Schwertmannite[1]	2,9	1,6	Epsomite	-3,2	-4,1
Schwertmannite[2]	0,3	-0,7	Gypsum	-1,3	-1,8
Goethite	4,2	4,5			
Hematite	10,3	10,9			
			Illite	-	-13,9
Basaluminite	-14,7	-8,3	Chlorite	-	-54,4
Gibbsite	-4,6	-2,5	Montmorillonite-Ca	-12,9	-9,0
Jurbanite	0,0	0,0	Kaolinite	-7,7	-4,2
Al(OH)3	-6,6	-4,5	Quartz	0,3	-0,1
			Albite	-12,9	-11,4

1. Ks from Yu et al. (1999)
2. Ks from Bigham et al. (1996)

Table 2. Summary of saturation indices (SI) obtained from geochemical calculations with PHREEQC code (Parkhurst and Appelo, 1999). The event values are the mean of the saturation indices of individual samples.